

# Pyrazolopyrimidines Establish MurC as a Vulnerable Target in *Pseudomonas aeruginosa* and *Escherichia coli*

Shahul Hameed P,<sup>†</sup> Praveena Manjrekar,<sup>†</sup> Murugan Chinnappattu,<sup>†</sup> Vaishali Humnabadkar,<sup>†</sup> Gajanan Shanbhag,<sup>†</sup> Chaitanyakumar Kedari,<sup>†</sup> Naina Vinay Mudugal,<sup>†</sup> Anisha Ambady,<sup>†</sup> Boudewijn L.M. de Jonge,<sup>‡</sup> Claire Sadler,<sup>§</sup> Beena Paul,<sup>†</sup> Shubha Sriram,<sup>‡</sup> Parvinder Kaur,<sup>†</sup> Supreeth Guptha,<sup>†</sup> Anandkumar Raichurkar,<sup>†</sup> Paul Fleming,<sup>‡</sup> Charles J. Eyermann,<sup>‡</sup> David C. McKinney,<sup>‡</sup> Vasana K. Sambandamurthy,<sup>†</sup> Manoranjan Panda,<sup>\*,†</sup> and Sudha Ravishankar<sup>\*,†</sup>

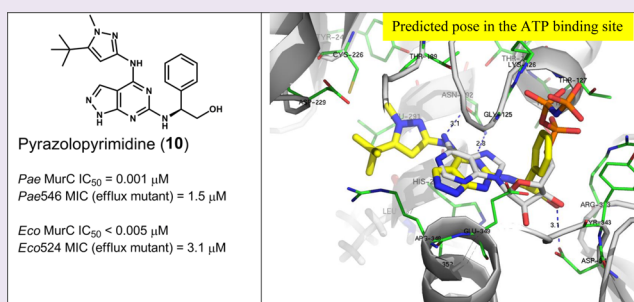
<sup>†</sup>Innovative Medicines, AstraZeneca India Pvt. Ltd., Bellary Road, Hebbal, Bangalore 560024, India

<sup>‡</sup>AstraZeneca Infection, Innovative Medicines, 35 Gatehouse Drive, Waltham, Massachusetts 02451, United States

<sup>§</sup>Global Safety Assessment, AstraZeneca, Alderley Park, Mereside, Cheshire, United Kingdom

## Supporting Information

**ABSTRACT:** The bacterial peptidoglycan biosynthesis pathway provides multiple targets for antibacterials, as proven by the clinical success of  $\beta$ -lactam and glycopeptide classes of antibiotics. The Mur ligases play an essential role in the biosynthesis of the peptidoglycan building block, *N*-acetylmuramic acid-pentapeptide. MurC, the first of four Mur ligases, ligates *L*-alanine to UDP-*N*-acetylmuramic acid, initiating the synthesis of pentapeptide precursor. Therefore, inhibiting the MurC enzyme should result in bacterial cell death. Herein, we report a novel class of pyrazolopyrimidines with subnanomolar potency against both *Escherichia coli* and *Pseudomonas aeruginosa* MurC enzymes, which demonstrates a concomitant bactericidal activity against efflux-deficient strains. Radio-labeled precursor incorporation showed these compounds selectively inhibited peptidoglycan biosynthesis, and genetic studies confirmed the target of pyrazolopyrimidines to be MurC. In the presence of permeability enhancers such as colistin, pyrazolopyrimidines exhibited low micromolar MIC against the wild-type bacteria, thereby, indicating permeability and efflux as major challenges for this chemical series. Our studies provide biochemical and genetic evidence to support the essentiality of MurC and serve to validate the attractiveness of target for antibacterial discovery.



The use of current antibacterial agents for the treatment of serious bacterial infections is severely limited due to the prevalence of drug resistant strains of bacteria across the globe. There is an urgent need to develop novel antibacterial agents to effectively tackle these serious bacterial infections.<sup>1</sup> Although there are several essential metabolic pathways in bacteria, most drugs in use and in development target only a few pathways and mechanisms such as DNA replication, protein synthesis, and cell wall biosynthesis.<sup>2,3</sup> Significant advances in genomics have resulted in the identification of a large number of essential targets in bacteria. Several high throughput screening efforts against these enzymes identified potent inhibitors, albeit with poor antibacterial activity. This highlights the difficulty in translating biochemical "target" potency into antibacterial activity.<sup>4,5</sup>

Peptidoglycan, an essential cell wall component of both gram-positive and gram-negative bacteria protects the cytoplasmic membrane from osmotic stress.<sup>6</sup> It is a glycopeptide polymer localized to the periplasmic space of bacteria and synthesized via a complex process divided into a cytoplasmic and an extracytoplasmic phase. Each of these biosynthetic

processes is comprised of multiple steps catalyzed by enzymes located either in the cytosol or on the inner membrane.<sup>7</sup> While the peptidoglycan building block, lipid II precursor is synthesized in a series of reactions in the cytoplasm, its polymerization and cross-linking in gram-negative species occurs in the periplasmic space.<sup>8,9</sup> Transpeptidases that catalyze the peptide cross-linking, the final step in the polymerization, are inhibited by the  $\beta$ -lactams and glycopeptides.<sup>10</sup> The clinical success of  $\beta$ -lactams and glycopeptides validates cell wall biosynthesis as a target of antibacterials;<sup>11</sup> however, the emergence and widespread resistance to these antibiotics globally has reignited the efforts to explore additional cell wall targets toward the discovery of novel antibacterial agents.<sup>12,13</sup> Recent advances in reconstructing the entire bacterial cell wall peptidoglycan biosynthetic pathway provide an attractive avenue to screen for new inhibitors of this process.<sup>14,15</sup> Some of these efforts have resulted in the

Received: May 9, 2014

Accepted: July 18, 2014

Published: July 18, 2014

identification of other cell wall biosynthesis inhibitors such as fosfomycin (MurA inhibitor) and D-cycloserine (D-Ala-D-Ala ligase/alanine racemase inhibitor).<sup>16,17</sup> The essential Mur ligases that catalyze the sequential addition of amino acids to build the pentapeptide on UDP-*N*-acetylmuramic acid (UNAM) are attractive targets for drug discovery, since no human homologues have been identified; this reduces the risk of target-based toxicity.<sup>18</sup> The Mur ligases build the pentapeptide in an energy-dependent manner by utilizing ATP to catalyze the amino acid transfer and thus are likely to share similar substrate binding pockets.<sup>19</sup> Earlier efforts reported to design or screen for inhibitors of either one of these Mur ligases or a combination of them have resulted in the identification of several enzyme inhibitors.<sup>20–25</sup> MurC, the first of Mur ligases, catalyzes the conversion of UNAM to UDP-*N*-acetylmuramoyl-L-alanine (UMA; Figure S1, Supporting Information). The enzyme has been purified to homogeneity,<sup>26</sup> and its tertiary and quaternary structures have been determined.<sup>27,28</sup> Several studies report the discovery of phosphinate substrate analogs, benzofuranacyl sulphonamide, 5-benzylidenethiazolidin-4-ones, and dihydro thienopyrazoles, as MurC inhibitors.<sup>20–23</sup> Additionally, feglymycin, a natural product comprising a 13-mer peptide was shown to inhibit both MurA and MurC of *E. coli* (*Eco*).<sup>29</sup> Unfortunately, none of these MurC inhibitors displayed antibacterial activity against either the wild-type or efflux-deficient strains of gram-negative bacteria with the exception of compound 3-(phenylethoxy)quinoxalin-2-amine (C1,<sup>22</sup>) which showed very poor activity (MIC = 64  $\mu$ g/mL) against a highly sensitized (*tolC* and *imp* mutated) strain. However, the study failed to establish if the observed antibacterial activity of C1 was due to the inhibition of MurC.<sup>22</sup>

Herein, we report the discovery and optimization of a hit series obtained from a high throughput screen of the AstraZeneca compound library against the *P. aeruginosa* (*Pae*) MurC enzyme. Structure–activity relationship (SAR) exploration on the original hit (pyrazolopyrimidine) resulted in the identification of a lead series with single digit nanomolar IC<sub>50</sub> against both *Eco* and *Pae* MurC enzymes and potent antibacterial activity against efflux-deficient strains of these bacterial species. The pyrazolopyrimidines were found to be bactericidal, and the mode of action studies in both *Eco* and *Pae* confirmed MurC as the molecular target. To our knowledge, this is the first report that demonstrates that inhibition of MurC leads to growth suppression, thereby establishing MurC as a valid target for antibacterial therapy.

## RESULTS AND DISCUSSION

**General Synthesis of Pyrazolopyrimidines (Scheme 1, Supporting Information S2).** Aromatic nucleophilic substitution of 4,6-dichloro pyrazolopyrimidine with commercially available aminopyrazoles (**IIa–IIId**) in the presence of sodium carbonate provided the mono-alkylated intermediates (**IIIa–IIId**) in good yield. The alkylation of intermediates **IIIa–IIId** with glycinol (**IV**) in the presence of sodium carbonate and Hunigs base under microwave irradiation led to compounds **1–19** in moderate yield. Carbamates **20–26** were readily obtained by reacting amines with the active carbamate formed by the reaction of compound **10** and carbonyl diimidazole. Compound **1** was identified as a hit from the high throughput screening against *Pae* MurC with an IC<sub>50</sub> of 1  $\mu$ M. The series was lead-like with desirable physicochemical properties. One of the potential challenges of this series could be the achievement of selectivity against human kinases.<sup>30</sup> Initial medicinal chemistry

efforts focused on improving the potency against *Pae* MurC. These led to a 100-fold improvement in IC<sub>50</sub> (Figure 1).

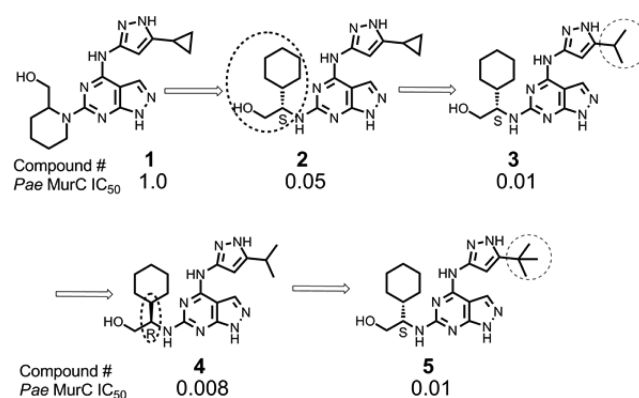


**Figure 1.** Initial SAR and improvement in enzymatic potency against *Pae* MurC enzyme. The IC<sub>50</sub> values are expressed in  $\mu$ M. The structural changes are encircled with dotted lines.

Replacing the piperidinyl methanol group with a cyclohexyl glycinol improved the potency 20-fold (Figure 1, matched pair 1:2). Substitution of the isopropyl and tertiary butyl group instead of cyclopropyl in the pyrazole ring led to further improvement in enzyme potency (matched pairs: 2:3:5). Furthermore, comparison of data from the enantiomers from the cyclohexyl glycinol chiral center indicated a slight preference for the R-isomer.

**Proposed Binding Mode of Pyrazolopyrimidines.** In the absence of a crystal structure, we built a homology model of *Pae* MurC based on the published cocrystal structure of *H. influenzae* (*Hin*) MurC (pdb ID: 1P3D)<sup>31</sup> (Supporting Information Figure S3-1). The sequence identity between *Hin* MurC and *Pae* MurC was found to be 57%, and the active site was conserved by >85% (Supporting Information Figure S3-2, Table S3-1). The model was validated using standard methods and minimized prior to docking (Supporting Information S3). The N-terminal domain (residues 1–115) harbors the UDP binding region, and it comprises of five stranded parallel  $\beta$ -sheets surrounded by four  $\alpha$ -helices. Residues 119–324, known as the central domain, present in all Mur ligases, constitute a major part of the ATP binding site. This has seven stranded parallel  $\beta$ -sheet surrounded by five helices. The central domain of the Mur ligases MurC, MurD, MurE, and MurF are topologically equivalent. The C-terminal domain (residues 325–480) has six stranded  $\beta$ -sheet flanked by 5  $\alpha$ -helices. This domain is broadly conserved across all Mur ligases and with some variation in length and orientation of helices and loops.

The key residues interacting with adenine, ribose, and phosphate units of stable ATP analog adenosine imidodiphosphate (ANP) are conserved between *Hin* MurC and *Pae* MurC. The refined homology model of *Pae* MurC reiterated these key interactions with ANP (Supporting Information, Figure S3-1), suggesting that the model is robust enough to predict the binding modes through docking studies. A set of pyrazolopyrimidines was docked in the ATP binding site by employing the Glide extra precision module from Schrodinger.<sup>32,33</sup> The crystal structure of *Hin* MurC with ANP<sup>31</sup> and site directed mutagenesis studies on *Eco* MurC<sup>34</sup> suggest that the hydrogen bonding contact with Asn292 (Asn295 in *Hin* MurC, Asn296 in *Eco* MurC) is one of the conserved interactions and is

considered as the warhead interaction for ligand binding. The predicted mode for monosubstituted pyrazole derivatives such as **5** suggests that the N-5 atom of pyrazolopyrimidine ring and the C-4 amine are engaged in H-bonding contacts with Asn292 (Figure 2). The pyrazolopyrimidine ring is flanked between the

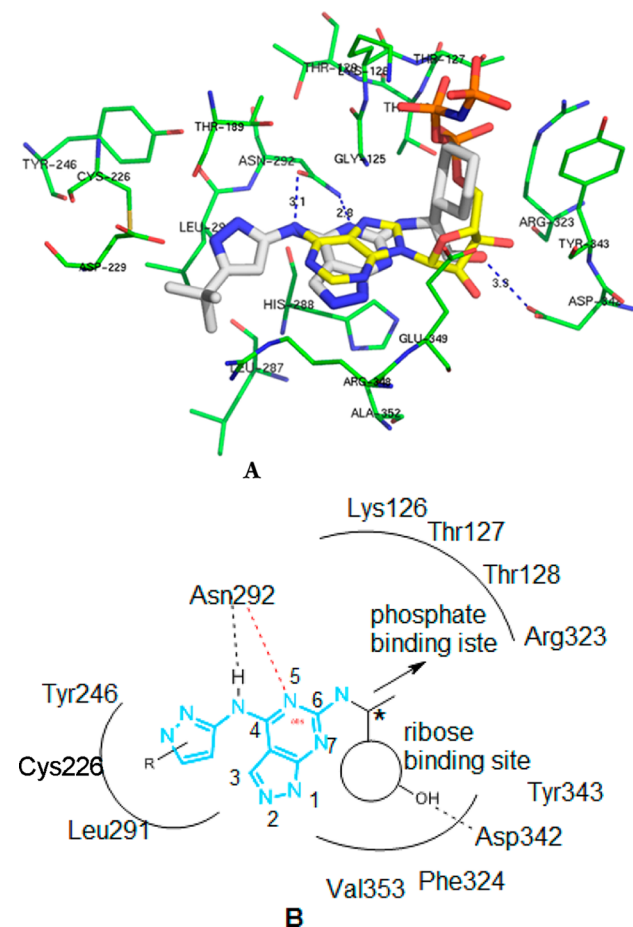
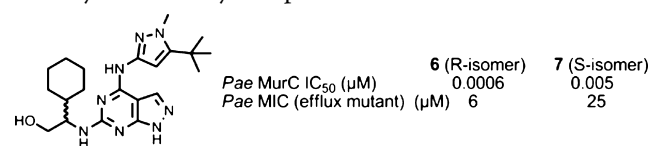


**Figure 2.** (A) Predicted binding mode of pyrazolopyrimidine (S, blue) in the *Pae* MurC active site. The crystal coordinates of adenosine (yellow) derived from the template structure is overlaid. (B) The 2D-depiction of the binding pocket and areas to grow and modify pyrazolopyrimidine scaffold are represented.

imidazole side chains of His288 and His124 that could potentially make CH- $\pi$  or  $\pi$ - $\pi$  interactions. The cyclohexyl group occupies the sugar pocket and the -OH group mimics the C2'-OH of ribose, interacting with Asp342. Additionally, the side chains of residues such as Val353, Phe324, and Arg323 can make hydrophobic contacts with the glycinol substituents. These favorable van der Waals contacts may be responsible for the remarkable improvement in potency observed when the piperidinyl methanol is replaced with cyclohexyl glycinol (matched pair 1:2). The overlay with adenosine imidodiphosphate (Figure 2A, yellow) suggests that the series can be suitably modified to grow toward the phosphate binding site.

The binding pocket occupied by the pyrazole ring revealed several interesting features that were exploited further to improve potency. The iPr (**3**, **4**) or tBu (**5**) groups are likely to make favorable van der Waals contacts while interacting with the hydrophobic side chains of Leu291, Cys226, and Tyr246. Substitution that led to a marked improvement in enzymatic activity was the replacement of methyl group at the free -NH

of the pyrazole ring (e.g., **6** and **7**). The preference for R-isomer for enzymatic activity was pronounced.



Docking of the disubstituted pyrazole derivative (e.g., **6** and **7**) suggested an alternate binding mode (Figure 3B) in addition

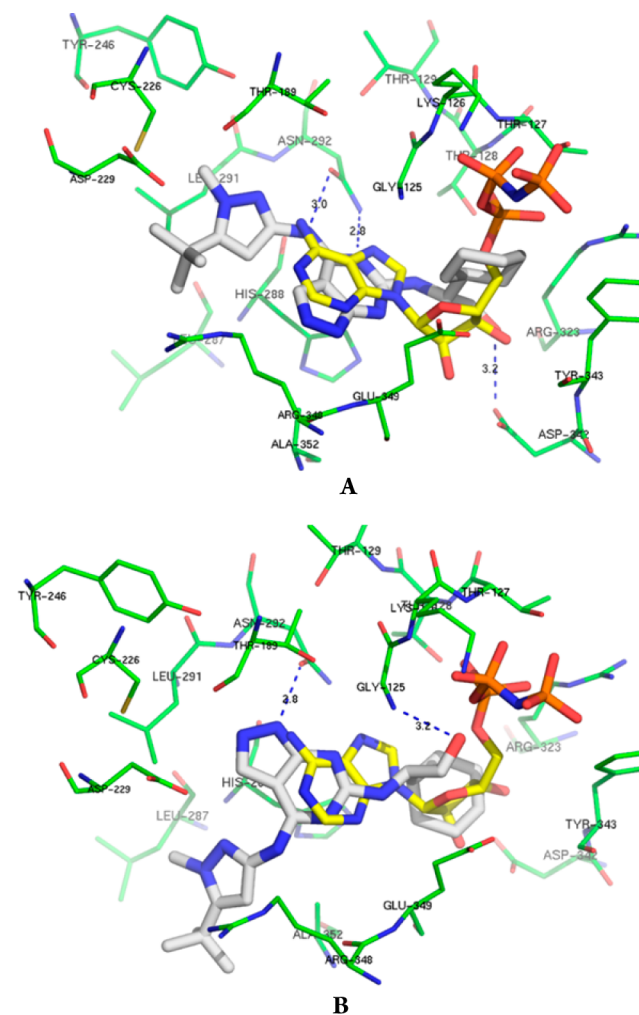


**Figure 3.** Two possible modes of binding for compound **6** (R-isomer). (A) The binding mode where amine linker and N5 of pyrimidine forms the warhead interaction with Asn292. (B) The alternate binding mode where pyrazolo N atom forms the contact with Asn292.

to the one described earlier. Figure 3A depicted the binding mode for **6** that was similar to the monosubstituted derivative **5** (Figure 2). As shown in Figure 3B, the warhead interaction of Asn292 was with the N1 atom of the pyrazolopyrimidine ring resulting in the disubstituted pyrazole unit being shifted. The methyl and tertiary butyl groups in both the predicted poses were making favorable van der Waals contacts with the side chains of hydrophobic residues (Tyr246, Cys226 in the case of A and Leu291, Arg348 in the case of B). It is interesting to note that in the case of pose B, the -OH group makes H-bond contact with Gly125 and is directed toward the phosphate binding site.



For the subsequent SAR exploration, the *t*-butyl, methyl substituted pyrazole was kept unchanged and the substituents directed toward the ribose binding site were explored with a *R*-enantiomer. A few key molecules are shown in Table 1.

Replacement of cyclohexyl group by tetrahydropyran or small isopropyl group showed 10–20 fold loss in activity (**8** and **9**). Aryl rings such as phenyl, pyridyl, and isoxazole (**10–12**, **14–15**, Table 1) exhibited very potent MurC inhibition ( $IC_{50} < 10$  nM). Constraining the glycinol side chain into amino indanol ring retained the single digit nanomolar potency. Limited exploration of substituted aryl rings (**16–19**, Table 1) retained the potency. These explorations indicated that the glycinol side chain is amenable for variety of substitutions that can be further explored to improve potency or modulate physicochemical properties.

The single digit nanomolar or subnanomolar inhibitors showed antibacterial activity against an efflux-deficient strain of *P. aeruginosa* (*Pae*546, see Supporting Information for strain description) and *E. coli* (*Eco*524). Compound **10** was found to have the best optimal balance with a *Pae* MurC  $IC_{50}$  of 1 nM and a *Pae*546 MIC of 1.6  $\mu$ M. No activity (MIC > 200  $\mu$ M) was seen against wild-type isolates (Supporting Information S4).

The challenge of getting antibacterial activity against the wild-type *Pae* strain remained elusive. The reasons could be due to a combination of poor compound permeability with multiple efflux mechanisms, many of which are unique to gram-negative pathogens,<sup>35,36</sup> especially *Pae*. The methods explored to circumvent these issues include increasing the polarity and ionic nature of the scaffold and introducing metal chelating siderophores.<sup>37,38</sup> Ionizable groups and siderophores were attached in the phosphate binding region to increase the chances of permeation through the outer membrane of the gram-negative pathogens. A few key compounds made and tested with these hypotheses are listed in Table 2 (compounds **20–26**). While subnanomolar enzymatic potency was mostly retained for these derivatives, antibacterial activity against the wild-type strains was not achieved (MIC > 200  $\mu$ M) (Supporting Information Table S4–1).

The inhibitory activity of a few representative compounds on *Eco* MurC was measured. The highly conserved active site between *Pae* MurC and *Eco* MurC was reflected in obtaining a good correlation between the  $IC_{50}$  for the two isozymes (Tables 1 and 2; the scatter plot showing the correlation between the  $IC_{50}$  is given in Supporting Information Figure S5–1).

Except for compounds **23** and **26**, wherein a single digit nanomolar inhibition against the enzyme did not translate into MIC, there was a good correlation in the series between MIC and enzymatic activity (Figure 4). These data suggest that pyrazolopyrimidines exhibit their MIC as a result of efficient target engagement with MurC enzyme within the bacterial cell.

**Selectivity against a Panel of Human Kinases.** One of our concerns with this scaffold was off target kinase activity. Single point screening of representative pyrazolopyrimidines against a panel of 40 kinases indicated this class has potent activity against some of the human kinases. Based on the single point data, a set of 16 kinases were selected for determining a dose response curve ( $IC_{50}$  measurement). The heat map derived from the  $IC_{50}$  measurement for a few representative pyrazolopyrimidines is shown in Figure 5.

The monosubstituted pyrazole derivatives (e.g., **3** and **5**) showed very potent activity against a number of kinases such as

**Table 1. SAR Modification for Ribose Site through Substituted Alicyclic and Heteroaromatic Rings**

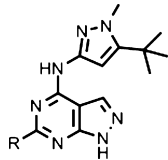
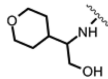
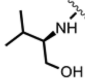
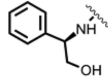
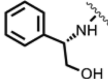
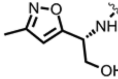
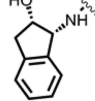
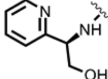
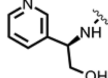
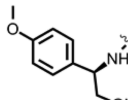
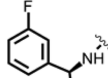
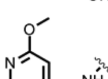
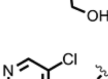
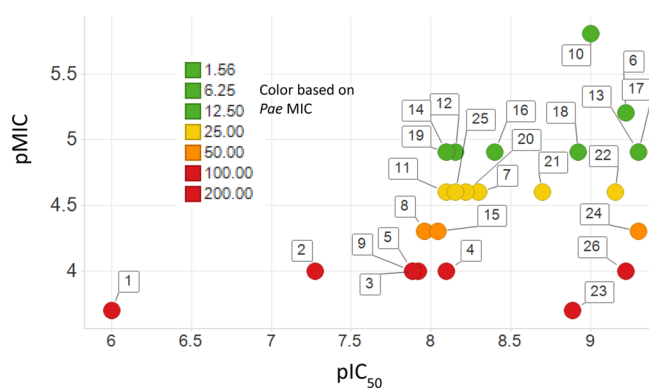
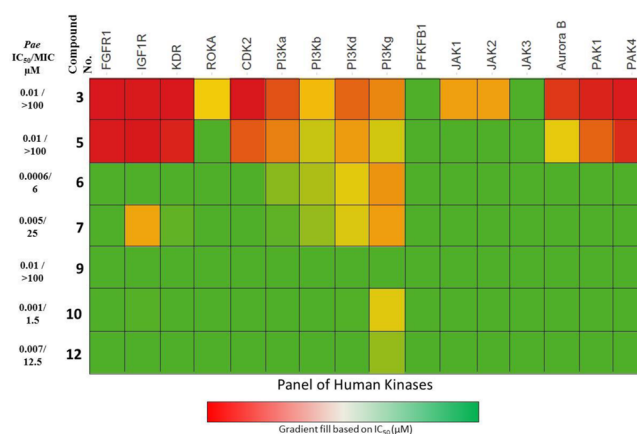
No	R=				
		<i>Pae</i> MurC $IC_{50}$ ( $\mu$ M)	<i>Eco</i> MurC $IC_{50}$ ( $\mu$ M)	<i>Pae</i> 546 MIC ( $\mu$ M)	<i>Eco</i> 524 MIC ( $\mu$ M)
<b>8</b>		0.011	0.101	50	100
<b>9</b>		0.013	0.188	>100	100
<b>10</b>		0.001	<0.005	1.56	3.13
<b>11</b>		0.008	0.011	25	200
<b>12</b>		0.007	0.060	12.5	25
<b>13</b>		<0.0005	0.002	12.5	12.5
<b>14</b>		0.008	0.040	12.5	100
<b>15</b>		0.009	nd	50	200
<b>16</b>		0.004	0.021	12.5	6.25
<b>17</b>		<0.0005	0.004	12.5	100
<b>18</b>		0.0012	0.015	12.5	12.5
<b>19</b>		0.008	0.057	12.5	25

Table 2. SAR Studies to Explore Putative Phosphate Binding Site

No	R2	Pae MurC IC <sub>50</sub> (μM)	Eco MurC IC <sub>50</sub> (μM)	Pae546 MIC (μM)	Eco524 MIC (μM)
20		0.006	0.052	25	200
21		0.002	0.003	25	50
22		0.0007	0.004	25	25
23		0.0013	<0.001	>200	>200
24		<0.0005	0.003	50	25
25		0.007	0.060	25	50
26		0.0006	0.005	100	12.5

Figure 4. Scatter plot of *Pae* MurC IC<sub>50</sub> (log scale) and *Pae*546 MIC against efflux-deficient mutant (log scale).

FGFR, CDK2, Aurora B2, PI3Ks, JAK1, JAK2, PAK1, and PAK2. However, for the disubstituted pyrazole derivatives (e.g., 6, 7, 9, 10, and 12), the potency against most of the kinases were found to be weak or very weak. For compound 10 (*Pae* MurC IC<sub>50</sub> = 1 nM and *Pae*546 MIC = 1.6 μM), the IC<sub>50</sub> values against all the kinases tested except for PI3K were found to be >30 μM (Figure 5). This data highlights that selectivity can be

Figure 5. Heat map generated from IC<sub>50</sub> data against a panel of human kinases. IC<sub>50</sub> > 30 μM are colored green. A yellow–orange–red gradient is used for data points with IC<sub>50</sub> < 30 μM.

achieved against human kinases while retaining the inhibitory potency against *Pae* MurC.

Representative pyrazolopyrimidines showed good selectivity against a human A549 cell line and no hERG cardiac channel inhibition at 33 μM. Most of the compounds from this class exhibited solubility >100 μM with >10% free fraction in a human plasma protein binding assay (Supporting Information Table S6-1). In general, compounds within this series with log D < 3 showed good solubility and higher free fractions in the human plasma protein binding assay.

**Mode of Action of Pyrazolopyrimidines.** To establish the molecular mechanism of action, a multipronged approach involving biochemical, metabolic labeling and genetic methods was employed. The availability of compounds with a low micromolar MIC against the efflux-deficient mutant with good solubility enabled us to probe the molecular target. All of the experiments described below were performed in an efflux-deficient strain of *Eco* and *Pae*.

**Precursor Incorporation Studies.** We employed a standard radio-labeled precursor incorporation assay in *E. coli* *lysA*<sup>−</sup> *tolC*<sup>−</sup> strain in the presence of different concentrations of compounds 6 and 10, as previously reported.<sup>39</sup> We found compounds 6 and 10 to specifically inhibit the incorporation of <sup>3</sup>H-DAP into *E. coli* *lysA*<sup>−</sup> *tolC*<sup>−</sup> cells with an IC<sub>50</sub> of 4.4 and 0.7 μM, respectively. In contrast, the incorporation of other radio-labeled precursors such as <sup>3</sup>H-thymidine, <sup>3</sup>H-uracil were unaffected even at 80 times higher compound concentration (Supporting Information Table S7-1). This data suggested that pyrazolopyrimidines exert their action via inhibition of peptidoglycan biosynthesis. As peptidoglycan biosynthesis is a multistep process, we employed a MurC overexpressing strain along with classical genetics to gain further insight into the molecular mechanism of action.

**Loss of MIC in MurC Overexpression Strains.** *E. coli* *tolC*<sup>−</sup> (*Eco*524) strains hyper expressing either *Eco* or *Pae* *murC* gene under the control of an arabinose inducible promoter were generated (Supporting Information S8).

A set of representative pyrazolopyrimidines when tested against *Eco*524 strain overexpressing *Eco* MurC exhibited at least an 8-fold elevation in the MIC values, while the *Pae* MurC overexpressing strain did not show such a high degree of MIC modulation (only 4-fold MIC shift observed for most compounds; Supporting Information Table S8-1). Protein expression analysis of the *Eco* MurC and *Pae* MurC

overexpressing strains without and with induction using 0.4% arabinose provided an explanation for the less pronounced MIC modulation in the *Pae* MurC overexpressing strain. The recombinant strain with a plasmid carrying *Eco* MurC upon induction with 0.4% arabinose displayed a substantial increase in the expression of MurC protein, which was not the case with *Pae* MurC, as seen in a coomassie stained protein gel (Supporting Information Figure S8-1). The increase in MIC observed in the recombinant strains overexpressing *Eco* MurC in conjunction with the precursor incorporation data provided proof for target engagement of MurC by pyrazolopyrimidines in *E. coli*.

#### Resistance Mutation Maps to *murC* gene in *Pae*546.

To further explore the genetic basis of resistance to pyrazolopyrimidines, we generated spontaneous resistant mutants in an efflux-deficient strain of *Pae* (*Pae*546) followed by resistance mutation mapping. As a first step, the minimum bactericidal concentration (MBC) was determined to be within 4-fold of MIC concentration for compounds **6** and **10** (data not shown). Spontaneous resistant mutants arose at a low frequency of  $10^{-9}$  when bacterial cells were exposed to compound containing plates (at 4× and 8× MIC concentrations). In order to establish the specificity of these resistant mutants, random mutants were screened for their MIC against compounds **6**, **10**, their close analogs, and a few reference inhibitors. The resistant mutants exhibited a 8-fold shift in their MIC against the parent compound and no shift in their MIC against reference inhibitors (Table 3). These data suggested

**Table 3. MIC Modulation Against the Resistant Mutants of Compounds **6** and **10****

inhibitor	MIC ( $\mu$ M) <i>Pae</i> 546	MIC ( $\mu$ M) 10 <sup>8</sup> P8N1 (Y246C)	MIC ( $\mu$ M) 10 <sup>8</sup> P16N1 (Y246C)	MIC ( $\mu$ M) 6 <sup>8</sup> P4N1 (R151W)
linezolid	12.5	12.5	25	25
erythromycin	6.3	6.3	6.3	3.1
meropenem	0.06	0.06	0.06	0.1
ampicillin	250	250	250	>250
ofloxacin	0.02	0.02	0.02	0.008
<b>6</b>	6.2	>200	>200	50
<b>10</b>	12.5	>200	>200	100
<b>20</b>	3.1	>200	>200	25

that the resistant mutants are likely to harbor specific mutations in the target, rather than mutations in efflux or permeability genes. Given the significant structural similarity at the active site of Mur ligases, we decided to sequence the *murC*, along with the *murD*, *murE*, and *murF* genes from the genomic DNA of resistant mutants. In the resistant mutants raised to compound **6**, we observed two single point mutations in the *murC* gene, resulting in a R151W or N182R (data not shown) amino acid substitution in several independent resistant clones. In resistant mutants raised to compound **10**, a single point mutation in the *murC* gene resulted in a Y246C amino acid substitution in several independent resistant clones. All the observed mutations are part of the central ATP binding domain of MurC. Arg151 is part of a loop in the ATP binding domain; however, it is 8.5 Å away from the closest ligand atom (phosphate of the ATP). The mutation Y246C observed for compound **10** resistant mutants support the predicted pose on the basis of the homology model. The amino acid Tyr246 makes a van der Waal's contact with the tertiary butyl group attached to the pyrazole ring of pyrazolopyrimidines.

No mutations were observed either in the *murD* or *murE* or *murF* genes in these resistant mutants. This data provided conclusive proof that the pyrazolopyrimidines suppress bacterial growth via inhibition of MurC in *Pae*546. The comparative studies of ATP and substrate binding sites of Mur ligases from *E. coli*<sup>40</sup> have revealed several interesting differentiating features. While the ATP binding site is fairly conserved, the conformational changes required to carry out the reaction with increasing substrate size as we go from MurC to F can be striking and may lead to specific inhibitors. Hence, the specificity noted for pyrazolopyrimidine toward MurC is not surprising. The remarkable improvement in MurC IC<sub>50</sub> obtained from a small modification in the scaffold (Figure 1) and the enantiomeric preference (Figure 2) are indicative of the specific features of MurC active site. Further biochemical studies against MurD, E, and F would lead to a better understanding of the selectivity shown by pyrazolopyrimidines.

This is the first report of chemical validation of the essentiality and vulnerability of MurC in a gram-negative pathogen demonstrated via a combination of biochemical, precursor incorporation, and genetic approaches.

**Colistin Treatment Brings in Wild-Type MIC.** Encouraged by the potent IC<sub>50</sub> and the clear demonstration of target engagement, we probed if the lack of MIC for pyrazolopyrimidines in wild-type *E. coli* strain was due to the permeability barriers in the bacteria. A number of studies have utilized colistin for its cell permeabilizing property to demonstrate synergy under both *in vitro* and *in vivo*<sup>41–43</sup> conditions. The MIC for few pyrazolopyrimidines, peptidoglycan inhibitors, and protein synthesis inhibitor was tested against *E. coli* K12 wild-type strain pre-exposed to a subinhibitory concentration of colistin. Peptidoglycan inhibitors such as ramoplanin, tunicamycin, vancomycin, fosfomycin, bacitracin, and nisin showed significant MIC reductions in this assay, whereas ampicillin did not show any MIC modulation (Table 4). This data suggests

**Table 4. MIC ( $\mu$ M) of *E. coli*-K12 Strain Pre-exposed to Colistin**

inhibitor	MIC without colistin exposure ( $\mu$ M)	MIC with colistin exposure ( $\mu$ M)	target enzyme
ramoplanin	>50	0.4	MurG
nisin	>38	2.4	MurG
ampicillin	11	5.7	transpeptidase
bacitracin	>89	0.7	lipid pyrophosphorylase
fosfomycin	22	2.7	MurA
tunicamycin	>76	0.6	MraY
vancomycin	88	0.1	transpeptidase
<b>12</b>	>50	12.5	MurC
<b>13</b>	>50	3.1	MurC
<b>22</b>	>25	1.5	MurC
<b>26</b>	>25	1.5	MurC

that the difference in MIC observed is due to the changes in the permeability of the bacterial cell post exposure to colistin. The pyrazolopyrimidines also exhibited a significant improvement in their MIC following a brief exposure to colistin. Further studies are warranted to investigate the potential of combining pyrazolopyrimidines with suitable partner drugs known to improve permeability to deliver an attractive novel agent to treat serious bacterial infections.



In conclusion, we report the discovery of pyrazolopyrimidines as novel inhibitors of the *Eco* and *Pae* MurC. A detailed medicinal chemistry effort aided by molecular modeling resulted in the identification of specific inhibitors of MurC that are selective against a panel of human kinases. Further lead optimization efforts culminated in achieving sub-nanomolar enzyme inhibitors with appreciable antibacterial activity against efflux-deficient mutants of *Eco* and *Pae*. By employing a combination of biochemical, precursor labeling and genetic studies, we firmly established the target link to MurC. The lack of activity against wild-type bacteria could be attributed to permeability and efflux barriers in the bacterial cell. This observation was confirmed by achieving MIC in efflux-deficient mutants and by pretreatment with colistin. To the best of our knowledge, this is the first report of a potent small molecule MurC inhibitor targeting gram-negative pathogens with demonstrated antibacterial activity. Further lead optimization efforts to mitigate the permeability challenge and combination studies in the presence of advanced permeabilizing agents<sup>44</sup> will unravel the full potential of the series as an antibacterial agent.

## METHODS

**General Chemical Methods.** All commercial reagents and solvents were used without further purification. Analytical thin-layer chromatography (TLC) was performed on SiO<sub>2</sub> plates on alumina. Visualization was accomplished by UV irradiation at 254 and 220 nm. Flash column chromatography was performed using the Biotage Isolera flash purification system with SiO<sub>2</sub> 60 (particle size 0.040–0.055 mm, 230–400 mesh). Purity of all final derivatives for biological testing was confirmed to be >95% as determined using the following conditions: a Shimadzu HPLC instrument with a Hamilton reverse phase column (HxSil, C18, 3  $\mu$ m, 2.1 mm  $\times$  50 mm (H<sub>2</sub>)). Eluent A: 5% CH<sub>3</sub>CN in H<sub>2</sub>O. Eluent B: 90% CH<sub>3</sub>CN in H<sub>2</sub>O. A flow rate of 0.2 mL/min was used with UV detection at 254 and 214 nm. The structure of the intermediates and end products was confirmed by <sup>1</sup>H NMR and mass spectroscopy. Proton magnetic resonance spectra were determined in DMSO-*d*<sub>6</sub> unless otherwise stated, using Bruker DRX 300 or Bruker DRX-400 spectrometers, operating at 300 or 400 MHz, respectively. Splitting patterns are indicated as follows: s, singlet; d, doublet; t, triplet; m, multiplet; br, broad peak. LCMS data was acquired using Agilent LCMS VL series. Source: ES ionization, coupled with an Agilent 1100 series HPLC system and an Agilent 1100 series PDA as the front end. HRMS data was acquired using an Agilent 6520, Quadrupole-Time of flight tandem mass spectrometer (Q-ToF MS/MS) coupled with an Agilent 1200 series HPLC system.

Detailed experimental procedures for the synthesis and the associated analytical data of intermediates and final compounds are provided in the Supporting Information.

## ASSOCIATED CONTENT

### Supporting Information

Biochemical reactions carried out by Mur ligases including MurC; chemistry; molecular modeling; antibacterial activity of compounds against wild-type *Pae* and *Eco* strains; IC<sub>50</sub> correlation between *Pae* and *Eco* MurC; safety and DMPK profile; precursor incorporation studies; MIC modulation in MurC overexpression strains; generation and characterization of spontaneous resistant mutants; colistin exposure to determine the MIC in wild-type *E. coli* K12 strain; MurC protein purification and assays to determine IC<sub>50</sub>; plasmids and strains used. This material is available free of charge via the Internet at <http://pubs.acs.org>.

## AUTHOR INFORMATION

### Corresponding Authors

\*Email: [sudha.ravi40@rediffmail.com](mailto:sudha.ravi40@rediffmail.com).

\*Email: [manapanda@gmail.com](mailto:manapanda@gmail.com).

### Author Contributions

S.H.P. and M.P. are responsible for medicinal chemistry design and analyses. P.M., G.S., M.C., C.K., and D.M. are responsible for synthetic chemistry. J.E., A.R., and M.P. designed and performed the modeling. V.H. designed, performed, and analyzed the IC<sub>50</sub> determination experiments. S.S. and B.d.J. designed and performed the precursor incorporation experiments. S.R. and V.K.S. designed and analyzed the mode of action (MoA) studies. N.V.M. and A.A. performed MoA experiments. P.K. and S.G. performed and analyzed MIC determination. P.F. performed the hit triage for the high through screening output. S.R., M.P., and S.H.P. wrote the manuscript with contributions from all coauthors.

### Notes

The authors declare no competing financial interest.

## ACKNOWLEDGMENTS

We are thankful to S. Solapure and V. Ramachandran for the useful discussions regarding enzyme and microbiological assays, respectively. We thank N. Gao and S. Livchack for purification and supply of *Pae* MurC. We acknowledge the support and guidance from P. Warner, A. Dudley, V. Balasubramanian, R. Tommasi, A. Patten, and V. Hosagrahara during the course of this work.

## ABBREVIATIONS

*Pae*: *Pseudomonas aeruginosa*; *Eco*: *Escherichia coli*; MurC: UDP-N-acetylmuramic acid:L-alanine ligase; *murC*: the gene encoding MurC; <sup>3</sup>H-DAP: tritiated diamino pimelic acid; MurNac-PP: UDP-N-acetylmuramyl pentapeptide; Mur: UDP-N-acetylmuramic acid; UNAM: UDP-N-acetylmuramic acid; UMA: UDP-N-acetylmuramoyl-L-alanine; *Hin*: *Haemophilus influenzae*; ANP: phosphoaminophosphonic acid–adenylate ester; FGFR: Fibroblast growth factor receptor; CDK: Cyclin-dependent kinase; PI3K: phosphoinositide 3-kinase; JAK: Janus (protein tyrosine) kinase; PAK: p21 activated kinases

## REFERENCES

- (1) Laxminarayan, R.; Duse, A.; Wattal, C.; Zaidi, A. K. M.; Wertheim, H. F. L.; Sumpradit, N.; Vlieghe, E.; Hara, G. L.; Gould, I. M.; Goossens, H.; Greko, C.; D So, A.; Bigdeli, M.; Tomson, G.; Woodhouse, W.; Ombaka, E.; Peralta, A. Q.; Qamar, F. N.; Mir, F.; Kariuki, S.; Bhutta, Z. A.; Coates, A.; Bergstrom, R.; Wright, G. D.; Brown, E. D.; and Cars, O. (2013) Antibiotic resistance—The need for global solutions. *Lancet Infect. Dis.* 13, 1057–1098.
- (2) Kohanski, M. A., Dwyer, D. J., and Collins, J. J. (2010) How antibiotics kill bacteria: from targets to networks. *Nat. Rev. Microbiol.* 8, 423–425.
- (3) Butler, M. A.; Blaskovich, M. A.; and Cooper, M. A. (2013) Antibiotics in the clinical pipeline in 2013. *J. Antibiot. (Tokyo)* 66, 571–591.
- (4) Payne, D. J.; Gwynn, M. N.; Homes, D. J., and Pampliano, D. L. (2007) Drugs for bad bugs: Confronting the challenges of antibacterial discovery. *Nat. Rev. Drug Discovery* 6, 29–40.
- (5) Silver, L. L. (2011) Challenges of Antibacterial Discovery. *Clin. Microbiol. Rev.* 24, 71–109.
- (6) Vollmer, W., and Seligman, S. J. (2010) Architecture of peptidoglycan: More data and more models. *Trends Microbiol.* 18, 59–66.

- (7) Vollmer, W., and Bertsche, U. (2008) Murein (peptidoglycan) structure, architecture, and biosynthesis in *Escherichia coli*. *Biochim. Biophys. Acta* 1778, 1714–1734.
- (8) Barreateau, H., Kovac, A., Boniface, A., Sova, M., Gobec, S., and Blanot, D. (2008) Cytoplasmic steps of peptidoglycan biosynthesis. *FEMS Microbiol. Rev.* 32, 168–207.
- (9) Heijenoort, J. V. (2001) Formation of glycan chains in the synthesis of bacterial peptidoglycan. *Glycobiology* 11, 25–36.
- (10) Oka, T., Hashizume, K., and Fujita, H. (1980) Inhibition of peptidoglycan transpeptidase by  $\beta$ -lactam antibiotics: Structure–activity relationships. *J. Antibiot. (Tokyo)* 33, 1357–1362.
- (11) Bush, K. (2012) Antimicrobial agents targeting bacterial cell walls and cell membranes. *Rev. Sci. Technol.* 31, 43–56.
- (12) Voets, G. M., Platteel, T. N., Fluit, A. C., Scharringa, J., Schapendonk, C. M., Stuart, J. C., Bonten, M. J., and Hall, M. A. (2012) Population distribution of  $\beta$ -lactamase conferring resistance to third-generation cephalosporins in human clinical enterobacteriaceae in The Netherlands. *PLoS One* 7, e52102.
- (13) Courvalin, P. (2006) Vancomycin resistance in gram-positive cocci. *Clin. Infect. Dis.* 42, S27.
- (14) Zapun, A., Philippe, J., Abrahams, K. A., Signor, L., Roper, D. I., Breukink, E., and Vernet, T. (2013) In vitro reconstitution of peptidoglycan assembly from the gram-positive pathogen *Streptococcus pneumoniae*. *ACS Chem. Biol.* 8, 2688–2696.
- (15) Sheng, J., Huang, L., Zhu, X., Cai, J., and Xu, Z. (2014) Reconstitution of the peptidoglycan cytoplasmic precursor biosynthetic pathway in cell-free system and rapid screening of antisense oligonucleotides for Mur enzymes. *Appl. Microbiol. Biotechnol.* 98, 1785–1794.
- (16) Raz, R. (2011) Fosfomycin: An old—new antibiotic. *Clin. Microbiol. Infect.* 18, 4–7.
- (17) Prosser, G. A., and de Carvalho, L. P. (2013) Reinterpreting the mechanism of inhibition of *Mycobacterium tuberculosis* D-alanine:D-alanine ligase by D-cycloserine. *Biochemistry* 52, 7145–7149.
- (18) Kotnik, M., Anderluh, P. S., and Prezeli, A. (2007) Development of novel inhibitors targeting intracellular steps of peptidoglycan biosynthesis. *Curr. Pharm. Des.* 13, 2283–2309.
- (19) Ikeda, M., Wachi, M., Jung, H. K., Ishino, F., and Matsunashi, M. (1990) Homology among MurC, MurD, MurE, and MurF proteins in *Escherichia coli* and that between *Escherichia coli* MurG and a possible MurG protein in *Bacillus subtilis*. *J. Gen. Appl. Microbiol.* 36, 179–187.
- (20) Tomas, T., Zidar, N., Kovac, A., Turk, S., Mihael Simčič, M., Blanot, D., Iler-Premru, M. M., Filipic, M., Grdadolnik, S. G., Zega, A., Anderluh, M., Gobec, S., Kikelj, D., and Mašič, L. P. (2010) 5-Benzylidenethiazolidin-4-ones as multitarget inhibitors of bacterial Mur ligases. *ChemMedChem* 5, 286–295.
- (21) Tomašič, T., Šink, R., Zidar, N., Fic, A., Martel, C. C., Dessen, A., Patin, D., Blanot, D., Gobec, S., Zega, A., Kikelj, D., and Mašič, L. P. (2012) Dual inhibitor of MurD and MurE ligases from *Escherichia coli* and *Staphylococcus aureus*. *ACS Med. Chem. Lett.* 3, 626–630.
- (22) Zawadzke, L. E., Norcia, M., Desbonnet, C. R., Wang, H., Freeman-Cook, K., and Dougherty, T. J. (2008) Identification of an inhibitor of the MurC enzyme, which catalyzes an essential step in the peptidoglycan precursor synthesis pathway. *Assay Drug Dev. Technol.* 6, 95–103.
- (23) Reck, F., Marmor, S., Fisher, S., and Wuonola, W. A. (2001) Inhibitors of the bacterial cell wall biosynthesis enzyme MurC. *Bioorg. Med. Chem. Lett.* 11, 1451–1454.
- (24) Guzman, J. D., Wube, A., Evangelopoulos, D., Gupta, A., Hüfner, A., Basavannacharya, C., Rahman, M., Thomaschitz, C., Bauer, R., McHugh, T. D., Nobeli, I., Prieto, J. M., Gibbons, S., Bucar, F., and Bhakta, S. (2011) Interaction of N-methyl-2-alkenyl-4-quinolones with ATP-dependent MurE ligase of *Mycobacterium tuberculosis*: Antibacterial activity, molecular docking, and inhibition kinetics. *J. Antimicrob. Chemother.* 66, 1766–1772.
- (25) Hrast, H., Turk, S., Sosi, I., Knez, D., Randall, C. P., Barreateau, H., Contreras-Martel, C., Dessen, A., O'Neill, A. J., Mengin-Lecreux, D., Blanot, D., and Gobec, S. (2013) Structure activity relationships of new cyanothiophene inhibitors of the essential peptidoglycan biosynthesis enzyme MurF. *Eur. J. Med. Chem.* 66, 32–45.
- (26) Zoeiby, A. E., Sanschagrin, F., Lamoureux, J., Darveau, A., and Levesque, R. C. (2000) Cloning, over-expression, and purification of *Pseudomonas aeruginosa* MurC encoding uridine diphosphate N-acetylmuramate:L-alanine ligase. *FEMS Microbiol. Lett.* 183, 281–288.
- (27) Zoeiby, A. E., Sanschagrin, F., and Levesque, R. C. (2003) Structure and function of the Mur enzymes: Development of novel inhibitors. *Mol. Microbiol.* 47, 1–12.
- (28) Jin, H., Emanuele, J. J., Jr., Fairman, R., Robertson, J. G., Hail, M. E., Ho, H. T., Falk, P. J., and Villafranca, J. J. (1996) Structural studies of *Escherichia coli* UDP-N-acetylmuramate:L-alanine ligase. *Biochemistry* 35, 1423–1431.
- (29) Rausch, S., Hänchen, A., Denisiuk, A., Löhken, M., Schneider, T., and Süßmuth, R. D. (2011) Feglymycin is an inhibitor of the enzymes MurA and MurC of the peptidoglycan biosynthesis pathway. *ChemBioChem* 12, 1171–1173.
- (30) Block, M. H., Han, Y., Josey, J. A., Lee, J. W., Scott, D., Wang, B., Wang, H., Wang, T., Yu, D. (2005) Preparation of pyrazole derivatives as inhibitors of receptor tyrosine kinases, *PCT Int. Appl. WO* 2005049033 A1 20050602.
- (31) Mol, C. D., Brooun, A., Dougan, D. R., Hilgers, M. T., Tari, L. W., Wijnands, R. A., Knuth, M. W., Mcree, D. E., and Swanson, R. V. (2003) Crystal structures of active fully assembled substrate- and product-bound complexes of UDP-N-acetylmuramic acid:L-alanine ligase (MurC) from *Haemophilus influenzae*. *J. Bacteriol.* 185, 4152–4162.
- (32) *Small-Molecule Drug Discovery Suite*. (2013) 2013-3: Glide, version 6.1, Schrödinger, LLC, New York, 20.
- (33) Friesner, R. A., Murphy, R. B., Repasky, M. P., Frye, L. L., Greenwood, J. R., Halgren, T. A., Sanschagrin, P. C., and Mainz, D. T. (2006) Extra precision glide: Docking and scoring incorporating a model of hydrophobic enclosure for protein–ligand complexes. *J. Med. Chem.* 49, 6177–6196.
- (34) Bouhss, A., Mengin-Lecreux, D., Blanot, D., van Heijenoort, J., and Parquet, C. (1997) Invariant amino acids in the Mur peptide synthetases of bacterial peptidoglycan synthesis and their modification by site-directed mutagenesis in the UDP-MurNAc:L-alanine ligase from *Escherichia coli*. *Biochemistry* 36, 11556–11563.
- (35) Bolla, J. M., Alibert-Franco, S., Handzlik, J., Chevalier, J., Mahamoud, A., Boyer, G., Kiec-Kononowicz, K., and Pages, J. M. (2011) Strategies for bypassing the membrane barrier in multidrug resistant gram-negative bacteria. *FEBS Lett.* 585, 1682–1690.
- (36) Savage, P. B. (2001) Multidrug-resistant bacteria: Overcoming antibiotic permeability barriers of gram-negative bacteria. *Ann. Med.* 33, 167–171.
- (37) Faraldo-Gomez, J. D., and Sansom, M. S. P. (2003) Acquisition of siderophores in gram-negative bacteria. *Nat. Rev. Mol. Cell Biol.* 4, 105–116.
- (38) Moellmann, U., Heinisch, L., Bauernfeind, A., Koehler, T., and Ankel-Fuchs, D. (2009) Siderophores as drug delivery agents: Application of the “Trojan horse” strategy. *BioMetals* 22, 61–75.
- (39) Buurman, E. T., Johnson, K. D., Kelly, R. K., and MacCormack, K. (2006) Different modes of action of naphthyridones in gram-positive and gram-negative bacteria. *Antimicrob. Agents Chemother.* 50, 1385–1387.
- (40) Smith, C. A. (2006) Structure, function, and dynamics in the mur family of bacterial cell wall ligases. *J. Mol. Biol.* 362, 640–655.
- (41) Gordon, N. C., Png, K., and Wareham, D. W. (2010) Potent synergy and sustained bactericidal activity of a vancomycin-colistin combination versus multidrug-resistant strains of *Acinetobacter baumannii*. *Antimicrob. Agents Chemother.* 54, 5316–5322.
- (42) Karaoglan, I., Zer, Y., Bosnak, V. K., Mete, A. O., and Namiduru, M. (2013) *In vitro* synergistic activity of colistin with tigecycline or  $\beta$ -lactam antibiotic/ $\beta$ -lactamase inhibitor combinations against carbapenem-resistant *Acinetobacter baumannii*. *J. Int. Med. Res.* 41, 1830–1837.
- (43) Hornsey, M., and Wareham, D. W. (2011) *In vivo* efficacy of glycopeptide-colistin combination therapies in a *Galleria mellonella*



model of *Acinetobacter baumannii* infection. *Antimicrob. Agents Chemother.* 55, 3534–3537.

(44) Lamers, R. P., Cavallari, J. F., and Burrows, L. L. (2013) The efflux inhibitor phenylalanine-arginine  $\beta$ -naphthylamide (PA $\beta$ N) permeabilizes the outer membrane of gram-negative bacteria. *PLoS One* 8, e60666.